JACS
JOURNAL OF THE AMERICAN CHEMICAL SOCIETY
pubs.acs.org/JACS
Article

Proximity Histidine Labeling by Umpolung Strategy Using Singlet Oxygen

Keita Nakane, Shinichi Sato,* Tatsuya Niwa, Michihiko Tsushima, Shusuke Tomoshige, Hideki Taguchi, Minoru Ishikawa, and Hiroyuki Nakamura

Cite This: https://doi.org/10.1021/jacs.1c01626
Read Online
ACCESS | Metrics & More | Article Recommendations | Supporting Information

ABSTRACT: While electrophilic reagents for histidine labeling have been developed, we report an umpolung strategy for histidine functionalization. A nucleophilic small molecule, 1-methyl-4-arylurazole, selectively labeled histidine under singlet oxygen ($^1O_2$) generation conditions. Rapid histidine labeling can be applied for instant protein labeling. Utilizing the short diffusion distance of $^1O_2$ and a technique to localize the $^1O_2$ generator, a photocatalyst in close proximity to the ligand-binding site, we demonstrated antibody Fc-selective labeling on magnetic beads functionalized with a ruthenium photocatalyst and Fc ligand, ApA. Three histidine residues located around the ApA binding site were identified as labeling sites by liquid chromatography−mass spectrometry analysis. This result suggests that $^1O_2$-mediated histidine labeling can be applied to a proximity labeling reaction on the nanometer scale.

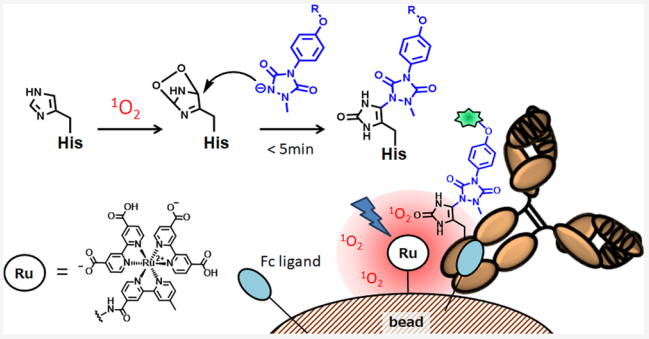

INTRODUCTION

Irreversible covalent bond formation with natural proteins is a powerful approach for the analysis of living systems and the creation of novel protein-based biomaterials. Modifying nucleophilic lysine and cysteine amino acid residues using electrophiles such as *N*-hydroxysuccinimide and maleimide is used widely as a traditional method for functionalizing purified proteins. Although this method has contributed greatly to life science research to expand the protein functionalization toolbox, protein labeling methods targeting less nucleophilic amino acid residues have gained attention in recent years.[1,2] Furthermore, reactions using highly reactive species have evolved as an alternative approach in the past decade. In recent years, many methods have utilized a technique called proximity-dependent labeling (PDL), in which a highly reactive chemical species is generated by an enzyme or a small catalyst molecule, and the surrounding environment is selectively labeled. PDL has emerged as a powerful approach for mapping protein−protein interactions, spatial transcriptomes, and site-selective protein labeling. Highly reactive species such as radicals,[3−7] carbene,[8,9] metallocarbene,[10] and activated electrophilic species[11] have been reported.

Singlet oxygen ($^1O_2$) is a highly reactive oxygen species that can be generated by light irradiation of a photocatalyst. As the possible diffusion distance of $^1O_2$ is only ∼10 nm,[12] spatially restricted oxidation can be controlled around the photocatalyst. Chromophore-assisted laser inactivation (CALI), in which $^1O_2$ is produced by photoirradiation of the photocatalyst, inactivates the target molecules and their assembled molecules in living cells.[13] Switchable photooxygenation catalysts that selectively produce $^1O_2$ on aggregated proteins have also been reported.[14−16] In $^1O_2$-mediated protein labeling, disulfide bond formation with a free cysteine residue (−SH) has been reported;[17] however, the target of this method is largely limited due to the low abundance of free cysteine residues and their low solvent accessibility. Although methods of nucleophilic trapping of amino acid residues by $^1O_2$ oxidation have been reported, it remains unclear which amino acid residues were modified, probably because of their low reaction efficiencies.[18,19] Histidine residues are one of the major targets of $^1O_2$-induced oxidation. Diels−Alder addition of $^1O_2$ to the histidine imidazole ring yields an endoperoxide intermediate, which is a reactive electrophile. Cross-linking reactions between the oxidized histidine and the nucleophilic amino acid residues under the $^1O_2$ generation condition have been reported;[20,21] however, there is no efficient labeling reagent that traps oxidized histidine species. Histidine is an attractive target amino acid in recent studies, and only a few histidine-selective labeling methods have been reported.[22,23] In

Received: February 9, 2021

this study, we found 1-methyl-4-arylurazole (MAUra) to be an efficient and selective trapper of oxidized histidine under $^1O_2$ generation conditions (Figure 1). Earlier methods utilize the

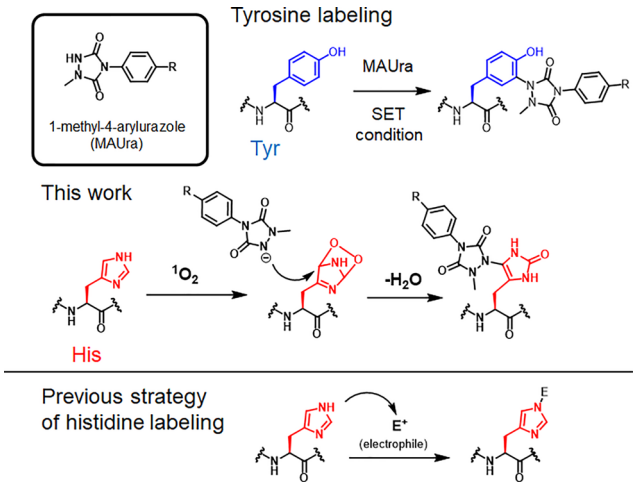

Figure 1. 1-Methyl-4-arylurazole labels not only tyrosine residues under the SET condition but also histidine residues under the $^1O_2$ generation condition.

nucleophilicity of histidine residues, whereas the current method is an umpolung strategy that utilizes the electrophilic property of the histidine oxidative intermediate generated by the reaction with $^1O_2$. Conversely, we also previously reported that MAUra labels tyrosine residues under the single-electron transfer (SET) condition.[24,25] Using a ruthenium photocatalyst, which catalyzes both $^1O_2$ generation and SET,[26,27] two different types of spatially restricted oxidative reactions, we performed photocatalyst-proximity labeling for site-selective labeling of the antibody Fc region.

RESULTS AND DISCUSSION

Inspired by the cross-linking between oxidized histidine and nucleophilic amino acid residues,[20,21] we thought that nucleophilic small molecules would be efficient labeling reagents to trap oxidized histidine. Therefore, we evaluated candidate labeling reagents that can modify a His-containing peptide (**1**: DRVAIHPF) under $^1O_2$ generation condition with Rose Bengal (Figures S1 and S2 in Supporting Information). Compared with known protein labeling reagents of oxidized proteins by $^1O_2$,[18,19] 1-methyl-4-phenylurazole (**2**)[24] showed the highest conversion efficiency. The reaction was completed by irradiation with light-emitting diode (LED) light for 10 min in the presence of Rose Bengal (Figure 2 and Figure S3). Due to the high nucleophilicity of the hydrazide structure[28] and the pK_a of 4.7,[29] the anion form of nucleophile **2** was considered to efficiently trap oxidized histidine. Since this reaction proceeded even under a direct $^1O_2$ generator without light irradiation, it suggested that the reaction was mediated by $^1O_2$ (Figure S4). To estimate the mechanism of labeling, **2** was added after the peptide was oxidized under the $^1O_2$ generation conditions, but no labeling was observed (Figure S5), suggesting that **2** traps short-lived electrophilic active species such as histidine endoperoxide[30] (Figure 1). The reaction efficiency reached a plateau (32%) within 3 min (Figure S6). Only specific amino acid residues (methionine, tryptophan, tyrosine, cysteine, and histidine side chains) have been found to undergo oxidation by $^1O_2$ under photooxidative conditions.[31] The reactions were

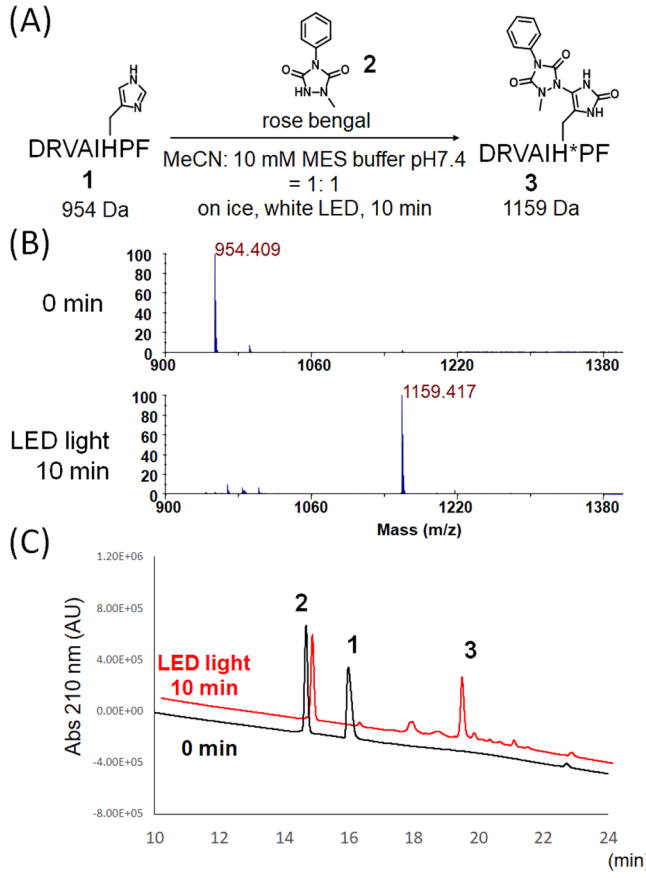

Figure 2. $^1O_2$-mediated histidine labeling. (A) Scheme of peptide labeling with **2**. (B) Matrix-assisted laser desorption ionization time of flight mass spectrometry analysis of crude samples. (C) High-performance liquid chromatography analysis of the labeling reaction. Peak **3** was also determined by tandem mass spectrometry analysis after separation (see Figure S3).

examined with peptides containing these amino acid residues, but no addition of **2** was observed for residues other than histidine, suggesting that the labeling was selective for histidine (Figure S7). Several peptides were labeled to compare the efficiency of oxidation and labeling reactions. As a result, it was found that methionine and tryptophan are oxidized under the reaction conditions that generate $^1O_2$ (Figures S8–S11). To determine the binding mode, Fmoc-His-OMe was used as a substrate, and the chemical structure of the product was analyzed by NMR spectroscopy. An oxygen atom was added to the C2 position of the imidazole ring, resulting in a urea structure, and a covalent bond was formed between the nitrogen atom of **2** and the C5 position of the imidazole ring (Figures S12–S15). Despite the short reaction time (10 min), the yield was 46%, which is comparable to the contemporary method of histidine labeling in which long reaction times (>3 h)[23] and basic conditions[22] are needed.

In addition to Rose Bengal, type II photosensitizers, $^1O_2$ generators such as methylene blue and ruthenium photocatalyst (48%) also catalyzed histidine labeling (Figure S16). We also labeled the peptide with azide-conjugated MAUra **4** and ruthenium photocatalyst and introduced a fluorescent group. Based on the fluorescence intensity, the yield was 50% (Figure S17). We hypothesized that the ruthenium photocatalyst would dual-label both histidine and tyrosine residues because it catalyzes both SET and $^1O_2$ generation, as described

https://doi.org/10.1021/jacs.1c01626
J. Am. Chem. Soc. XXXX, XXX, XXX−XXX

above.[27] We also performed protein labeling using bovine serum albumin (BSA) in the presence of **2** and $Ru(bpy)_3Cl_2$ under light irradiation. The labeled BSA was digested in a sodium dodecyl polyacrylamide gel electrophoresis (SDS-PAGE) gel. With nanoLC-MS/MS (liquid chromatography/tandem mass spectrometry) analysis of the peptide fragments, labeling of Y137 and H18 was detected (Figures S18 and S19). The oxidation reaction under these conditions was detected by MS analysis, suggesting that the exposed tyrosine and histidine residues were oxidized (Figure S20). For other small protein applications, ubiquitin containing a single histidine and a single tyrosine residue was also successfully labeled (Figures S21 and S22). To demonstrate the proximity labeling effect of the ligand-linked ruthenium catalyst, the GST-HaloTag was labeled. The catalytic efficiency of the HaloTag ligand-conjugated ruthenium photocatalyst was much higher than that of $Ru(bpy)_3Cl_2$, and a histidine residue in close proximity to the HaloTag ligand binding site was detected as a labeling site (Figures S23 and S24).

We developed beads functionalized with photocatalysts and ligands. Selective purification and tyrosine labeling of a target protein in a protein mixture were achieved simultaneously on the bead surface.[32] We also developed catalyst-proximity-dependent labeling using MAUra on beads functionalized with a ruthenium/4,4′-dicarboxybipyridine (dcbpy) complex and ligand.[7,32] Focusing on the immunoglobulin G (IgG) antibody size of 10 nm, a labeling radius of a few nanometers to 10 nm for SET and $^1O_2$ diffusion, antibody Fc region-selective labeling with MAUra on beads functionalized with ruthenium/dcbpy complex and Fc-binding ligand were performed. Unlike ligand-directed approaches for Fc-selective labeling,[33−36] in the current method, catalyst removal and antibody purification can be performed easily at the same time as labeling because the Fc ligand and catalyst are immobilized on magnetic beads.

Magnetic affinity beads functionalized with the Fc ligand and ruthenium/dcbpy (ligand/Ru beads) were synthesized. Fc-binding peptide[35,37] and small molecule ApA,[38] a non-peptidyl mimic of protein A, were selected as Fc ligands (Figure 3A). Trastuzumab, a humanized anti-human epithelial growth factor receptor type 2 (HER2) monoclonal antibody, was labeled using beads. After being labeled with azide-conjugated MAUra **4**, a fluorescent group was introduced to label the antibody using copper-free click chemistry with dibenzocyclooctyne-conjugated Cy3 (DBCO-Cy3). Labeled antibodies were evaluated for labeling efficiency by SDS-PAGE under non-reducing conditions. ApA-functionalized beads were found to catalyze antibody labeling more efficiently than the nonligand beads (Figure 3B). In contrast, almost no effect of the peptide ligand was observed in the case of peptide-functionalized beads. This was likely a result of the size of the peptide ligand; as the labeling radius by MAUra is a few nanometers from the bead surface, it seems necessary to use a small molecule Fc ligand in this case. The ligand and the catalyst on the bead surface were functionalized in very close proximity to each other. Although the calculation does not consider the thickness of the bead polymer phase, the average distance is about 0.4 nm, which is calculated from the loading amount of ligand and catalyst (Figure S25), the bead size (Dyna beads MyOne: 1.0 μm), and density (1.8 g/cm^3). To evaluate the site selectivity of the labeling reaction, antibodies were digested with papain and separated into Fab and Fc regions by SDS-PAGE (see Figure S26). Fc-selective labeling was observed using ApA/Ru

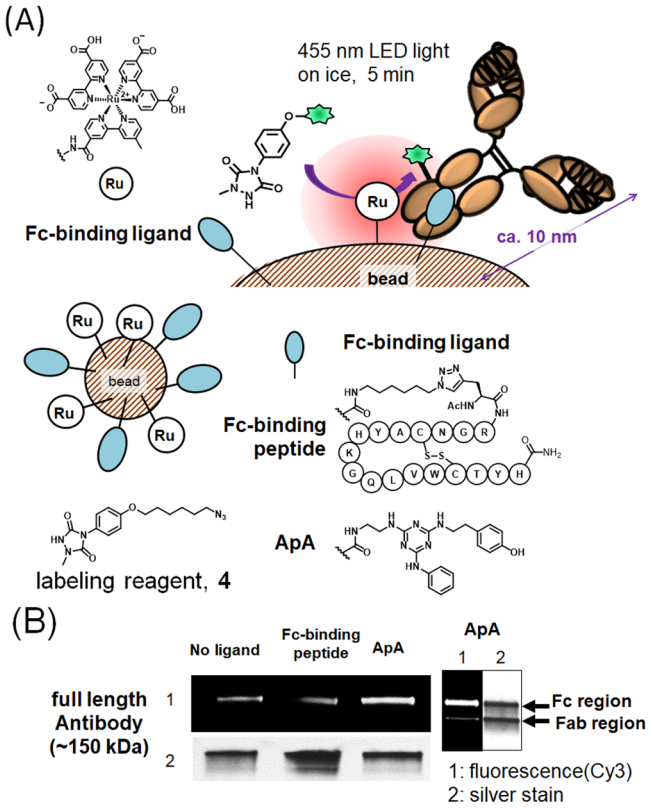

Figure 3. Proximity-dependent protein labeling on beads. (A) Fc-selective labeling on bead functionalized with ruthenium/dcbpy complex and Fc-binding ligand. Structures of beads functionalized with Ru/dcbpy and small molecule ligands (see Supporting Information Figure S25 for immobilized amounts of molecules on beads). (B) Evaluation of labeling efficiencies and Fc selectivities. Left: Full-length trastuzumab under the nonreductive conditions. No ligand: Beads functionalized with only Ru/dcbpy. Fc-binding peptide: Beads functionalized with Ru/dcbpy and Fc-binding peptide. ApA: Beads functionalized with Ru/dcbpy and ApA. Right: Papain-digested fragments of labeled trastuzumab labeled with ApA/Ru beads.

beads (Figure 3B). Although we also evaluated other types of small molecule Fc ligands, ApA/Ru beads showed the highest labeling efficiency and Fc selectivity (Figure S27).

The oxidation reaction by $^1O_2$ and the trapping of the oxidized histidine intermediate were completed quickly, and the labeling efficiency reached a plateau within 5 min of light (455 nm) irradiation (Figure S29). Labeling was suppressed by the addition of an excess amount of free Fc ligand (amine-conjugated ApA) (Figure S30) and in elution buffer conditions in which the antibody Fc region did not bind to ApA-functionalized beads (Figure S31). These results suggest that the labeling reaction is enhanced in a catalyst-proximity environment via binding of the Fc region and ApA on the beads. In addition, when a protein mixture of BSA and trastuzumab was labeled with the beads, the antibody heavy chain containing the Fc region was selectively labeled (Figure S32). The antibody binding affinity and labeling catalytic activity of the beads were reusable, and these abilities were not inactivated even after five cycles (Figure S33).

It was calculated that 0.22 Cy3 molecules/antibodies were labeled in the antibody eluted from the beads (Figure S34). It was also confirmed that antigen-recognition activity was hardly impaired after labeling and elution (Figure S35). In HER2-positive cells, Cy3-labeled trastuzumab was localized in the cell

https://doi.org/10.1021/jacs.1c01626
J. Am. Chem. Soc. XXXX, XXX, XXX−XXX

membrane, suggesting it retained antibody-recognition activity, whereas no accumulation of labeled trastuzumab was observed in HER2-negative cells (Figure S36). The sites oxidized under this trastuzumab labeling condition were detected by MS in the same manner as in Figure S20, and histidine, tryptophan, and tyrosine residues were detected as oxidation sites. There was good agreement between the oxidized sites and labeled sites (Figure S37).

Subsequently, we identified which amino acid residues were labeled in the Fc region by mass spectrometry. The SDS-PAGE band corresponding to the heavy chain of Cy3-labeled trastuzumab was digested in a gel with trypsin, and the resulting peptide fragments were analyzed by LC-MS. Three labeling sites were identified by the detection of Cy3-labeled peaks (Figure 4A and Figures S38–S40). The nanoLC-MS/

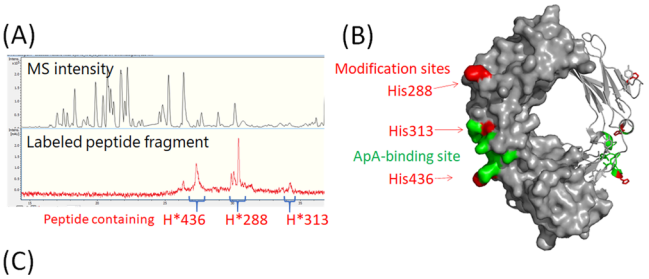

(C)

Residue	His438	His313	His436	His432	His288	His271
Distance (Å)	8.3	8.4	10.8	14.6	26.0	47.5
Solvent accessibility (Å^2)	39	27	129	0	115	71

Figure 4. Identified labeling sites. (A) LC analysis of labeled peptide fragments. (B) 3D structure of trastuzumab Fc region, labeled histidine residues (red), and ApA binding site (green) (PDB: 3D6G). The surface is displayed for one chain. (C) Table of distance from the ligand-binding site and side chain solvent accessibility of histidine residues in the Fc region of trastuzumab. See Figure S42 for distance calculations. Side chain solvent accessibilities (Å^2) were estimated by Discovery Studio 4.1 and in X-ray crystal structure of the trastuzumab Fc region (PDB: 3D6G).

MS analysis after digestion of **2**-labeled trastuzumab with trypsin and Glu-C revealed three labeling sites: H288, H313, and H436 (Figure 4B and Figure S41). Based on the positional relationship between the labeled sites and reaction field on the beads, labeling efficiencies were presumed to depend on both the distance from the ApA-binding site and the surface exposure level (Figure 4C). The labeling of Tyr439, the tyrosine residue closest to the ApA binding site, was not detected. It is probable that Tyr439 is buried beneath His436, and the ruthenium photocatalyst is in an environment where His436 can be preferentially approached. Other tyrosine residues located far from the ApA binding site (>21 Å) with low solvent accessibility were also not labeled (Figure S43).

This technique should be applicable to various IgG antibodies, as the Fc region has a conserved sequence present in all types of IgG. Cetuximab and rituximab, humanized antiepidermal growth factor receptor (EGFR), and anti-CD20 antibodies were also labeled using the same method. As expected, the beads selectively labeled the Fc regions of the antibodies (Figure S44). Using rituximab, the binding sites were identified by nanoLC-MS/MS in the same manner as in the experiment with trastuzumab. Two histidine residues (H289 and H437 in rituximab) corresponding to trastuzumab H288 and H436 were labeled (Figure S45).

The protein A mimic was reported to bind not only to human IgG but also to rabbit IgG.[39] Rabbit polyclonal anti-V5 epitope was successfully labeled using the beads (Figure S44). Finally, we performed selective labeling of the Fc region while purifying the antibody from rabbit serum. Rabbit serum was mixed with beads to purify the antibody, followed by a labeling reaction. The antibody Fc region was selectively modified while enriching the antibody from the serum protein mixture (Figures S46 and S47).

CONCLUSIONS

We found that MAUra efficiently labeled histidine residues under $^1O_2$ generation conditions. To our knowledge, this is the first report of a histidine-selective nucleophilic protein labeling reagent targeting oxidized histidine by $^1O_2$. Utilizing the short diffusion distance of $^1O_2$, we demonstrated antibody Fc-selective labeling on magnetic beads functionalized with a ruthenium photocatalyst and Fc ligand, ApA. This method has the following advantages: (1) protein functionalization with a short reaction time of 5 min, (2) one-pot operation of both antibody enrichment and labeling, (3) application to all types of IgG (human and various animal IgGs), and (4) reusability of the beads. Three histidine residues located around the ApA binding site were identified by LC-MS analysis, suggesting that $^1O_2$-mediated histidine labeling can be applied to a proximity labeling reaction on the nanometer scale. Although the distance between the catalyst and the ligand was not precisely controlled on the bead surface in this study, future improvements in site selectivity and efficiency can be expected by designing reaction fields with homogeneous ligand–catalyst distances. Research into further applications, such as intracellular photocatalyst-proximity labeling, is currently in progress.

EXPERIMENTAL SECTION

Peptide Labeling Using a Photocatalyst. Labeling reagent (from a 100 mM stock solution in DMSO, final concentration 1 mM) and photocatalyst (from a 100 mM stock solution, final concentration 1 mM) were added to a solution of peptide (final concentration 100 μM or 1 mM) in 50% CH_3CN solution in 10 mM MES buffer (pH 7.4) in a 1.5 mL tube. The solution was distributed and irradiated with white light (white LED, ISL-150 × 150 H3WH4R, 8.0 ± 0.5 mW/cm^2, CCS Inc.) for 10 min on ice. The resulting solution was desalted using C18 pipet tips (Nikkyo Technos Co., Ltd.). The reaction mixture was diluted 10 times with 0.1% trifluoroacetic acid (TFA) and mixed with α-cyano-4-hydroxycinnamic solution (5.0 mg/mL solution in acetonitrile/0.1% aq TFA = 0.5 μL/0.5 μL), and the mixture was placed on a MALDI-TOF plate and dried at room temperature. The labeled peptides were detected by MALDI-TOF MS analysis (Bruker, UltrafleXtreme, or ABSCIEX TOF/TOFTM 5800).

Bead Preparation. Dynabeads (Dynabeads MyOne carboxylic acid, 400–800 nmol/mg carboxylate, Invitrogen, 4.0 mg) were washed with dimethylformamide (DMF) and dissolved in 800 μL of 200 mM *N*-hydroxysuccinimide (NHS)/DMF solution. EDCI·HCl (final concentration 200 mM) was added to the mixture, which was stirred for 2 h at room temperature, and the beads were washed with DMF to give NHS ester-functionalized Dynabeads (stored in isopropyl alcohol at −20 °C). The NHS ester-functionalized Dynabeads (1.0 mg) were washed three times with 200 μL of DMF. Amine-conjugated Ru/dcpby (from 10 mM solution in H_2O, final concentration 100 μM), amine-conjugated Fc ligand (from 10 mM solution in DMF, final concentration 100 μM), and NEt_3 (from 100 mM stock solution in DMF, final concentration 1 mM) (final concentration of beads: 5.0 mg/mL) were added and stirred at room temperature for 1 h, and the beads were washed three times with

https://doi.org/10.1021/jacs.1c01626
J. Am. Chem. Soc. XXXX, XXX, XXX–XXX

DMF (200 μL). After 1 M 4-aminobutanol solution was added in DMF, the mixture was stirred at room temperature for 1 h and the beads were washed three times with 200 μL of DMF and 200 μL of 50% MeOH.

Antibody Labeling Using Beads. The beads functionalized with ruthenium photocatalyst and ligand (0.25 mg) were suspended in the solution of 50 μL of 1 μM antibody in 10 mM MES buffer (pH 7.4). After incubation for 4 h at 4 °C, azide-conjugated labeling reagent **4** or **2** (from 100 mM solution in DMSO, final concentration 500 μM) was added to the beads. The solution was distributed and irradiated with blue light (RELYON, Twin LED light, 455 nm) for 5 min on ice.

Papain Digestion. An aqueous suspension of papain (5 μL from 10 mg/mL suspension) was diluted with digestion buffer (45 μL, PBS (pH 7.4) containing 10 mM cysteine, and 10 mM EDTA). The mixture was incubated for 10 min at 37 °C and used as the activated papain solution (1 mg/mL papain). The azide-labeled antibody beads prepared by the above-described method in 10 mM MES buffer (pH 7.4) were added to preactivated papain (from 1 mg/mL solution in digestion buffer, final concentration 0.3 mg/mL) and incubated for 1 h at 37 °C. The digestion reaction was quenched by adding aq H_2O_2 (from 10 mM solution in water to a final concentration of 3 mM).

LC-MS and NanoLC-MS/MS Analyses. Bands corresponding to labeled antibody heavy chains were separated, and the excised bands (~1 mm pieces) were cut. Gel pieces were transferred into microtubes, and 1 mL of water was added to the tubes and incubated at 37 °C for 10 min. The solution was removed, and the washing procedure was repeated three times. For destaining, 50% CH_3CN in 100 mM NH_4HCO_3(aq) was added, incubated at 37 °C for 10 min, and the solution was removed. CH_3CN was added to the tubes for dehydration and incubated at 37 °C for 10 min, after which the solution was removed. To the tubes was added 100 mM dithiothreitol in 100 mM NH_4HCO_3(aq) for Cys reduction and incubated at 37 °C for 30 min, after which the solution was removed. To the tubes was added 250 mM iodoacetamide in 100 mM NH_4HCO_3(aq) for Cys alkylation, followed by incubation at room temperature for 30 min in the dark and removal of the solution. Then, 100 mM NH_4HCO_3(aq) was added to the tubes and removed, followed by 50% CH_3CN in 100 mM NH_4HCO_3(aq). After the solution was removed, trypsin solution was added to each tube and incubated overnight at 37 °C. The resulting solution was quenched with aqueous TFA solution (final concentration: 0.1%) and desalted using C18 pipet tips (Nikkyo Technos Co., Ltd.). The desalted solution was subjected to LC-MS analysis. See Supporting Information for detailed LC-MS and nanoLC-MS/MS measurement conditions.

■ ASSOCIATED CONTENT

Supporting Information

The Supporting Information is available free of charge at https://pubs.acs.org/doi/10.1021/jacs.1c01626.

Experimental procedures and spectral data along with supporting data (PDF)

■ AUTHOR INFORMATION

Corresponding Author

Shinichi Sato − *Frontier Research Institute for Interdisciplinary Sciences and Graduate School of Life Sciences, Tohoku University, Aoba-ku, Sendai 980-8577, Japan;* orcid.org/0000-0002-8563-1658; Email: shinichi.sato.e3@tohoku.ac.jp

Authors

Keita Nakane − *Graduate School of Life Sciences, Tohoku University, Aoba-ku, Sendai 980-8577, Japan*

Tatsuya Niwa − *Cell Biology Center, Institute of Innovative Research, Tokyo Institute of Technology, Yokohama, Kanagawa 226-8503, Japan*

Michihiko Tsushima − *Laboratory for Chemistry and Life Science, Institute of Innovative Research, Tokyo Institute of Technology, Yokohama, Kanagawa 226-8503, Japan*

Shusuke Tomoshige − *Graduate School of Life Sciences, Tohoku University, Aoba-ku, Sendai 980-8577, Japan;* orcid.org/0000-0002-4948-5809

Hideki Taguchi − *Cell Biology Center, Institute of Innovative Research, Tokyo Institute of Technology, Yokohama, Kanagawa 226-8503, Japan;* orcid.org/0000-0002-6612-9339

Minoru Ishikawa − *Graduate School of Life Sciences, Tohoku University, Aoba-ku, Sendai 980-8577, Japan;* orcid.org/0000-0002-3937-2261

Hiroyuki Nakamura − *Laboratory for Chemistry and Life Science, Institute of Innovative Research, Tokyo Institute of Technology, Yokohama, Kanagawa 226-8503, Japan;* orcid.org/0000-0002-4511-2984

Complete contact information is available at: https://pubs.acs.org/10.1021/jacs.1c01626

Notes

The authors declare no competing financial interest.

■ ACKNOWLEDGMENTS

This work was partially supported by a research grant from The Tokyo Biochemical Research Foundation (TBRF) (to S.S.), Grant-in-Aid for Young Scientists (A) (15H05490 to S.S.), a Grant-in-Aid for Scientific Research (B) (19H02848 to S.S.), and a Grant-in-Aid for Chemistry for Multimolecular Crowding Biosystems (20H04699 to H.N.) from MEXT, Japan. We would like to thank Editage (www.editage.com) for English language editing.

■ REFERENCES

(1) deGruyter, J. N.; Malins, L. R.; Baran, P. S. Residue-Specific Peptide Modification: A Chemist's Guide. *Biochemistry* **2017**, *56* (30), 3863−3873.

(2) Szijj, P. A.; Kostadinova, K. A.; Spears, R. J.; Chudasama, V. Tyrosine Bioconjugation-an Emergent Alternative. *Org. Biomol. Chem.* **2020**, *18* (44), 9018−9028.

(3) Rhee, H. W.; Zou, P.; Udeshi, N. D.; Martell, J. D.; Mootha, V. K.; Carr, S. A.; Ting, A. Y. Proteomic Mapping of Mitochondria in Living Cells via Spatially Restricted Enzymatic Tagging. *Science* **2013**, *339* (6125), 1328−1331.

(4) Li, X.; Rees, J. S.; Xue, P.; Zhang, H.; Hamaia, S. W.; Sanderson, B.; Funk, P. E.; Farndale, R. W.; Lilley, K. S.; Perrett, S.; Jackson, A. P. New Insights into the DT40 B Cell Receptor Cluster Using a Proteomic Proximity Labeling Assay. *J. Biol. Chem.* **2014**, *289* (21), 14434−14447.

(5) Sato, S.; Nakamura, H. Ligand-Directed Selective Protein Modification Based on Local Single-Electro-Transfer Catalysis. *Angew. Chem., Int. Ed.* **2013**, *52* (33), 8681−8684.

(6) Sato, S.; Yoshida, M.; Hatano, K.; Matsumura, M.; Nakamura, H. *N*′-Acyl-*N*-methylphenylenediamine as a Novel Proximity Labeling Agent for Signal Amplification in Immunohistochemisty. *Bioorg. Med. Chem.* **2019**, *27* (6), 1110−1118.

(7) Tsushima, M.; Sato, S.; Niwa, T.; Taguchi, H.; Nakamura, H. Catalyst-Proximity Protein Chemical Labelling on Affinity Beads Targeting Endogenous Lectins. *Chem. Commun.* **2019**, *55* (88), 13275−13278.

(8) Kotani, N.; Gu, J.; Isaji, T.; Udaka, K.; Taniguchi, N.; Honke, K. Biochemical Visualization of Cell Surface Molecular Clustering in Living Cells. *Proc. Natl. Acad. Sci. U. S. A.* **2008**, *105* (21), 7405−7409.

(9) Geri, J. B.; Oakley, J. V.; Reyes-Robles, T.; Wang, T.; McCarver, S. J.; White, C. H.; Rodriguez-Rivera, F. P.; Parker, D. L.; Hett, E. C.; Fadeyi, O. O.; Oslund, R. C.; MacMillan, D. W. C. Microenvironment Mapping via Dexter Energy Transfer on Immune Cells. *Science* **2020**, *367* (6482), 1091−1097.
(10) Popp, B. V.; Ball, Z. T. Structure-Selective Modification of Aromatic Side Chains with Dirhodium Metallopeptide Catalysts. *J. Am. Chem. Soc.* **2010**, *132* (19), 6660−6662.
(11) Shiraiwa, K.; Cheng, R.; Nonaka, H.; Tamura, T.; Hamachi, I. Chemical Tools for Endogenous Protein Labeling and Profiling. *Cell Chem. Biol.* **2020**, *27* (8), 970−985.
(12) Sies, H.; Menck, C. F. M. Singlet Oxygen Induced DNA Damage. *Mutat. Res., DNAging: Genet. Instab. Aging* **1992**, *275*, 367−375.
(13) Jacobson, K.; Rajfur, Z.; Vitriol, E.; Hahn, K. Chromophore-Assisted Laser Inactivation in Cell Biology. *Trends Cell Biol.* **2008**, *18* (9), 443−450.
(14) Taniguchi, A.; Shimizu, Y.; Oisaki, K.; Sohma, Y.; Kanai, M. Switchable Photooxygenation Catalysts That Sense Higher-Order Amyloid Structures. *Nat. Chem.* **2016**, *8*, 974−982.
(15) Ni, J.; Taniguchi, A.; Ozawa, S.; Hori, Y.; Kuninobu, Y.; Saito, T.; Saido, T. C.; Tomita, T.; Sohma, Y.; Kanai, M. Near-Infrared Photoactivatable Oxygenation Catalysts of Amyloid Peptide. *Chem* **2018**, *4*, 807−820.
(16) Suzuki, T.; Hori, Y.; Sawazaki, T.; Shimizu, Y.; Nemoto, Y.; Taniguchi, A.; Ozawa, S.; Sohma, Y.; Kanai, M.; Tomita, T. Photo-Oxygenation Inhibits Tau Amyloid Formation. *Chem. Commun.* **2019**, *55* (44), 6165−6168.
(17) To, T.; Medzihradszky, K. F.; Burlingame, A. L.; Degrado, W. F.; Jo, H.; Shu, X. Photoactivatable Protein Labeling by Singlet Oxygen Mediated Reactions. *Bioorg. Med. Chem. Lett.* **2016**, *26* (14), 3359−3363.
(18) Li, Y.; Aggarwal, M. B.; Ke, K.; Nguyen, K.; Spitale, R. C. Improved Analysis of RNA Localization by Spatially Restricted Oxidation of RNA-Protein Complexes. *Biochemistry* **2018**, *57* (10), 1577−1581.
(19) Tamura, T.; Takato, M.; Shiono, K.; Hamachi, I. Development of a Photoactivatable Proximity Labeling Method for the Identification of Nuclear Proteins. *Chem. Lett.* **2020**, *49* (2), 145−148.
(20) Liu, M.; Zhang, Z.; Cheetham, J.; Ren, D.; Zhou, Z. S. Discovery and Characterization of a Photo-Oxidative Histidine-Histidine Cross-Link in IgG1 Antibody Utilizing ^{18}O-Labeling and Mass Spectrometry. *Anal. Chem.* **2014**, *86* (10), 4940−4948.
(21) Xu, C.-F.; Chen, Y.; Yi, L.; Brantley, T.; Stanley, B.; Sosic, Z.; Zang, L. Discovery and Characterization of Histidine Oxidation Initiated Cross-links in an IgG1 Monoclonal Antibody. *Anal. Chem.* **2017**, *89* (15), 7915−7923.
(22) Jia, S.; He, D.; Chang, C. J. Bioinspired Thiophosphorodichloridate Reagents for Chemoselective Histidine Bioconjugation. *J. Am. Chem. Soc.* **2019**, *141* (18), 7294−7301.
(23) Chen, X.; Ye, F.; Luo, X.; Liu, X.; Zhao, J.; Wang, S.; Zhou, Q.; Chen, G.; Wang, P. Histidine-Specific Peptide Modification via Visible-Light-Promoted C-H Alkylation. *J. Am. Chem. Soc.* **2019**, *141* (45), 18230−18237.
(24) Sato, S.; Hatano, K.; Tsushima, M.; Nakamura, H. 1-Methyl-4-Aryl-Urazole (MAUra) Labels Tyrosine in Proximity to Ruthenium Photocatalysts. *Chem. Commun.* **2018**, *54* (46), 5871−5874.
(25) Sato, S.; Matsumura, M.; Kadonosono, T.; Abe, S.; Ueno, T.; Ueda, H.; Nakamura, H. Site-Selective Protein Chemical Modification of Exposed Tyrosine Residues Using Tyrosine Click Reaction. *Bioconjugate Chem.* **2020**, *31* (5), 1417−1424.
(26) Sato, S.; Morita, K.; Nakamura, H. Regulation of Target Protein Knockdown and Labeling Using Ligand-Directed Ru(bpy)$_3$ Photocatalyst. *Bioconjugate Chem.* **2015**, *26* (2), 250−256.
(27) Angerani, S; Winssinger, N. Visible Light Photoredox Catalysis Using Ruthenium Complexes in Chemical Biology. *Chem. - Eur. J.* **2019**, *25* (27), 6661−6672.
(28) Nigst, T. A.; Antipova, A.; Mayr, H. Nucleophilic Reactivities of Hydrazines and Amines: The Futile Search for the α-Effect in Hydrazine Reactivities. *J. Org. Chem.* **2012**, *77* (18), 8142−8155.
(29) Bausch, M. J.; David, B.; Dobrowolski, P.; Guadalupe-Fasano, C.; Gostowski, R.; Selmarten, D.; Prasad, V.; Vaughn, A.; Wang, L. H. Proton-Transfer Chemistry of Urazoles and Related Imides, Amides, and Diacyl Hydra-zides. *J. Org. Chem.* **1991**, *56* (19), 5643−5651.
(30) Liu, F.; Lu, W.; Fang, Y.; Liu, J. Evolution of Oxidation Dynamics of Histidine: Non-Reactivity in the Gas Phase, Peroxides in Hydrated Clusters, and pH Dependence in Solution. *Phys. Chem. Chem. Phys.* **2014**, *16* (40), 22179−22191.
(31) Grassi, L.; Cabrele, C. Susceptibility of Protein Therapeutics to Spontaneous Chemical Modifications by Oxidation, Cyclization, and Elimination Reactions. *Amino Acids* **2019**, *51*, 1409−1431.
(32) Tsushima, M.; Sato, S.; Nakamura, H. Selective Purification and Chemical Labeling of a Target Protein on Ruthenium Photocatalyst-Functionalized Affinity Beads. *Chem. Commun.* **2017**, *53* (35), 4838−4841.
(33) Kishimoto, S.; Nakashimada, Y.; Yokota, R.; Hatanaka, T.; Adachi, M.; Ito, Y. Site-Specific Chemical Conjugation of Antibodies by Using Affinity Peptide for the Development of Therapeutic Antibody Format. *Bioconjugate Chem.* **2019**, *30* (3), 698−702.
(34) Yamada, K.; Shikida, N.; Shimbo, K.; Ito, Y.; Khedri, Z.; Matsuda, Y.; Mendelsohn, A. B. AJICAP-Affinity Peptide Mediate Regiodivergent Functionalization of Native Antibodies. *Angew. Chem., Int. Ed.* **2019**, *58* (17), 5592−5597.
(35) Yamada, K.; Ito, Y. Recent Chemical Approaches for Site-Specific Conjugation of Native Antibodies: Technologies toward Next-Generation Antibody-Drug Conjugates. *ChemBioChem* **2019**, *20*, 2729−2737.
(36) Ohata, J.; Ball, Z. T. A Hexa-rhodium Metallopeptide Catalyst for Site-Specific Functionalization of Natural Antibodies. *J. Am. Chem. Soc.* **2017**, *139* (36), 12617−12622.
(37) Ito, Y. WO Patent Appl. 2016/186206 A1, 2016.
(38) Li, R.; Dowd, V.; Stewart, D. J.; Burton, S. J.; Lowe, C. R. Design, Synthesis, and Application of a Protein A Mimetic. *Nat. Biotechnol.* **1998**, *16*, 190−195.
(39) Teng, S. F.; Sproule, K.; Husain, A.; Lowe, C. R. Affinity Chromatography on Immobilized 'Biomimetic" Ligands Synthesis, Immobilization and Chromatographic Assessment of an Immunoglobulin G-Binding Ligand. *J. Chromatogr., Biomed. Appl.* **2000**, *740*, 1−15.

https://doi.org/10.1021/jacs.1c01626
J. Am. Chem. Soc. XXXX, XXX, XXX−XXX